Unfolding of Class A Amphipathic Peptides on a Lipid Surface†

Andrew H. A. Clayton,* Andra G. Vultureanu, and William H. Sawyer

Russell Grimwade School of Biochemistry and Molecular Biology, University of Melbourne, Parkville 3052, Victoria, Australia

Received June 26, 2002; Revised Manuscript Received October 2, 2002

ABSTRACT: The folding of polypeptides associated with biomembranes is a ubiquitous phenomenon, yet the thermodynamics underlying the process are poorly understood. In the present work we examine the unfolding of a series of α-helical amphipathic membrane-associated peptides using guanidine hydrochloride as a denaturant. The peptides are based on the class A amphipathic helix motif, and each contains a single tryptophan at sequence position 2, 3, 7, 12, or 14. The isothermal unfolding process was monitored by circular dichroism ellipticity at 222 nm to monitor changes in the helical structure of the peptide. Tryptophan fluorescence was used to probe the local changes in the environment about the indole fluorophore. The unfolding curves generated from the two experimental techniques for each peptide−lipid complex were noncoincident, suggesting the presence of stable intermediate(s) in the unfolding. A three-state model could adequately account for the data and yielded parameters which were consistent with the presence of a partially folded intermediate structure which (i) is closer in Gibb's free energy to the folded state than the unfolded state and (ii) retains much of the interfacial and amphipathic character of the folded state. Denaturant-induced peptide dissociation from the peptide−lipid complexes was found to be negligible as confirmed by size exclusion chromatography. The results are compared with related thermodynamic data and discussed in terms of current models of peptide folding at membrane interfaces.

The membrane insertion and folding of polypeptides in lipid bilayers continue to be an area of intense research activity (*1*, *2*). Both experimental and theoretical analyses support the notion that the lipid bilayer provides a unique solvent for the folding, insertion, and association of membrane polypeptides**.** Probing the kinetics and thermodynamics of transmembrane protein folding has proved difficult owing to the extreme insolubility of membrane proteins in the aqueous phase and their resistance to desorption/unfolding by temperature or by chemical denaturants within the lipid bilayer. Some model studies on transmembrane peptides and proteins, however, are bringing light to this important problem (*1*−*4*). For α-helical transmembrane proteins, such as ion channels and receptors, the folding and oligomerization can be usefully conceptualized as a two-stage process involving the formation of stable individual transmembrane α-helices and subsequent packing to form a functional protein (*1*).

There have been few quantitative studies of the unfolding/folding of proteins at a membrane interface (*5*). Water-soluble peptides that associate with membrane interfaces are in principle easier to study because they are smaller and can readily partition between the membrane and water phases. White and co-workers have developed a thermodynamic model for the interaction of peptides with interfaces that includes a contribution from partitioning of the unfolded polypeptide into the lipid interface and a contribution from the folding of the peptide at the interface (*5*). The results are largely consistent with the view that the folding of peptides at the membrane interface makes a large contribution to the overall peptide partitioning free energy owing to the high energetic cost of partitioning non-hydrogen-bonded peptide bonds into the interface (*5*−*8*). An understanding of the thermodynamics of folding at lipid interfaces is important since the formation of structural motifs, such as amphipathic α-helices, enables numerous peptide hormones, toxins, apolipoproteins, and antimicrobial peptides to associate with lipid bilayers.

In this study we make use of a set of membrane-associated 18-residue amphipathic α-helical peptides that possess a single tryptophan residue at sequence position 2, 3, 7, 12, or 14 (Figure 1). These peptides are representative of class A amphipathic helices found in apolipoproteins. We have made extensive use of the tryptophan fluorescence from these peptides as site-specific probes of tryptophan micropolarity (*10*), tryptophan rotamer distributions (*11*), and tryptophan motional dynamics at a phospholipid−bilayer interface (*12*). The results of this work, together with X-ray structural studies (*13*) carried out independently in the White laboratory, indicate that these peptides associate with the interface of lipid bilayers to form α-helices that align predominantly parallel to the membrane surface.

The purpose of the present paper is twofold. First, we wish to enquire whether an amphipathic peptide can exist or be induced to form a partially folded or unfolded state on a bilayer surface. Second, can we determine the thermodynam-

† Supported by the Australian Research Council. A.H.A.C. was a postdoctoral fellow of the Australian Research Council.

* Corresponding author. Current address: Ludwig Institute for Cancer Research, P.O. Box 2008, Royal Melbourne Hospital, Parkville, Victoria 3050, Australia. Phone: 61 3 9341 3155. Fax: 61 3 9347 1938. E-mail: Andrew.Clayton@ludwig.edu.au.

10.1021/bi020439z CCC: $25.00
Published on Web 01/22/2003

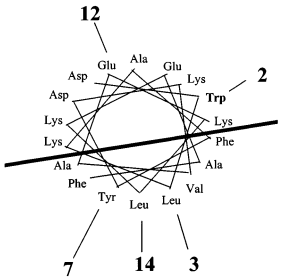

	Peptide
2	
DWLKAFYDKVAEKLKEAF	A-2
3	
DRWKAFYDKVAEKLKEAF	B-3
7	
DRLKAFWDKVAEKLKEAF	C-7
12	
DRLKAFYDKVAWKLKEAF	D-12
14	
DRLKAFYDKVAEKWKEAF	E-14

FIGURE 1: Helical wheel representation of 18-residue amphipathic peptides. The figures in bold refer to the positions of tryptophan substitution in peptides A-2, B-3, C-7, D-12, and E-14. The solid line represents the boundary between the hydrophilic and hydrophobic faces of the α-helix and allows identification of the two lysine residues at this interface that are a characteristic of class A amphipathic helices.

ics of the unfolding process at a lipid interface experimentally? We have examined the unfolding of class A amphipathic helices using GuHCl[1] as a denaturant, a method that can provide reasonable estimates of the conformational stability of proteins in solution and an indication of whether the unfolding is a single-step or multistep process (*9*). The isothermal unfolding induced by guanidine hydrochloride was monitored by circular dichroism, to determine changes in the secondary structure, and by tryptophan fluorescence, as a site-specific probe of local changes in the environment about the indole fluorophore in the peptide−lipid complexes. In addition, size-exclusion gel chromatography was used to determine whether the addition of denaturant affects the equilibrium between free and lipid-bound peptide states.

MATERIALS AND METHODS

Materials. Egg phosphatidylcholine (egg PC) was obtained as a chloroform−methanol stock solution from Lipid Products (U.K.) and used without further purification. The peptides were synthesized using Fmoc chemistry solid-phase synthesis and purified by HPLC as described previously (*10*). The five peptides based on the 18A sequence have a tryptophan residue substituted at position 2, 3, 7, 12, or 14 (A-2, B-3, C-7, D-12, and E-14, respectively) as indicated in Figure 1. Peptide concentrations were determined from the peptide absorption spectra using a molar extinction coefficient at 280 nm of 5690 M^{-1} cm^{-1} for peptide C-7 and 6950 M^{-1} cm^{-1} for peptides A-2, B-3, D-12, and E-14 (*1*). The buffer used in all experiments was 20 mM Na_2HPO_4, pH 7.4, and was filtered through a 0.45 μm Millipore filter before use. For gel chromatography experiments, 0.02% NaN_3 was added to the buffer as an antibacterial. Guanidine hydrochloride (GuHCl, 98% pure) was from BDH Chemicals Ltd. (England). Sephadex G-25 (medium) was from Pharmacia Biotech AB (Sweden).

Methods. Small unilamellar egg PC vesicles (egg PC SUVs) were prepared by sonication as described previously (*10*). Solutions for circular dichroism (CD) and fluorescence experiments were prepared by incubating the peptide with egg PC vesicles for 15 min prior to the addition of 8 M GuHCl to provide final concentrations of 0−1.4 M GuHCl. The final peptide concentration was 0.045 mg/mL (22 μM), and the peptide to lipid molar ratio was 1:200 (lipid concentration, 4.5 mM).

CD spectra were measured at 25 °C with an AVIV Model 62 DS spectrometer and 1 mm path length quartz cuvettes. The monitoring wavelength was 222 nm, and an integration time of 30 s was used per measurement. The results were corrected by subtracting the signal of a blank sample containing identical concentrations of lipid and GnHCl but no peptide. A plateau in corrected ellipticity values was observed for GnHCl concentrations >1.4 M. Further increases in background by addition of excess GnHCl did not alter the corrected ellipticities, suggesting that the background subtraction procedure was adequate. No time dependence of the spectroscopic signal was observed over a period of 6 h.

Fluorescence experiments were performed with a Perkin-Elmer LS-5 fluorometer. Emission spectra were recorded in the 300−500 nm range with excitation at 295 nm and using excitation and emission slit widths of 2 and 3 nm, respectively, and a scan speed of 60 nm/min. The signals were corrected for background scattering from the lipid and GuHCl as for the CD measurements.

Gel filtration chromatography experiments were carried out on a column (19 × 1 cm) of Sephadex G-25 (medium grade) and a flow rate of 1 mL/min. The mobile phase was 20 mM Na_2HPO_4 and 0.02% NaN_3, pH 7.4, containing the appropriate concentration of GuHCl (0, 0.2, 0.4, 1.4, or 4 M GuHCl). Before each sample (740 μL) was loaded, the column was equilibrated with 3 column volumes of the buffered GuHCl solution. Samples contained 22 μM peptide and 4.5 mM egg PC. Fractions (0.8 mL) were collected and analyzed for the presence of peptide using the intrinsic tryptophan fluorescence (λ_{ex} = 295 nm, λ_{em} = 350 nm).

Fluorescence resonance energy transfer measurements of peptide C-7 to diphenylhexatriene-doped egg PC SUVs were performed in the presence and absence of 1.4 M GuHCl. To prepare the doped vesicles, an aliquot (21 μL) of a diphenylhexatriene stock solution (2.2 mM in tetrahydrofuran) was added to freshly prepared egg PC SUVs and equilibrated with mixing for 3 h to allow complete uptake (as monitored by fluorescence of the diphenylhexatriene). No change in lipid probe emission was observed upon addition of GuHCl to peptide-free vesicles. The energy transfer efficiency was determined from the sensitized acceptor emission from the diphenylhexatriene in the presence of peptide C-7. The energy transfer efficiency value was combined with the average lifetime of the tryptophan residue in the absence of diphenylhexatriene to calculate the apparent average rate of energy transfer.

Data Analysis. Fluorescence and circular dichroism data were normalized to reflect the fraction of unfolded peptide as a function of denaturant concentration, and the curves were fitted to a three-state equilibrium model using Matlab software (MathWorks Inc., MA). Algorithms for the nonlinear analysis were kindly provided by Dr. Allen Minton (NIH, Bethesda). The fractional signal change, S[D], associated with unfolding of the peptide is given by the spectroscopic signal (fluorescence or CD) of the folded form of the peptide (X_i, at [D] = 0), the signal when the peptide is unfolded (X_f, at [D] = plateau value), and the signal observed

[1] Abbreviations: CD, circular dichroism; GuHCl, guanidine hydrochloride; egg PC, egg yolk phosphatidylcholine; SUVs, small unilamellar vesicles.

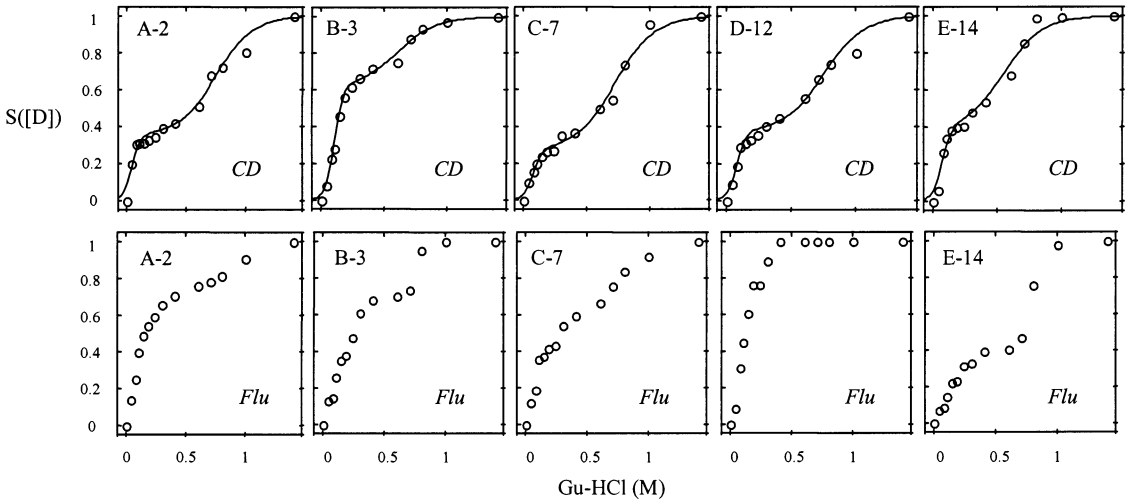

FIGURE 2: GuHCl-induced unfolding of amphipathic peptides A-2 to E-14 bound at the surface of unilamellar egg PC vesicles (lipid:peptide molar ratio 200:1, 20 °C, phosphate buffer, pH 7.4). The fractional signal change in circular dichroism ellipticity (upper panels) or fluorescence (lower panels) is plotted as a function of denaturant concentration. Solid lines represent the fits to a three-state denaturant binding model using the parameters in column 1 of Table 1.

at intermediate denaturant concentrations X[D]:

$$S([D]) = (X[D] - X_i)/(X_f - X_i) \quad (1)$$

Data were analyzed in terms of a three-state equilibrium involving a folded (N), unfolded (U), and intermediate (I) state:

$$N \underset{K_{ni}}{\rightleftharpoons} I \underset{K_{iu}}{\rightleftharpoons} U$$

where K_{ni} and K_{iu} are the equilibrium constants for the successive equilibria. The apparent overall equilibrium constant is K_{nu}. The fraction of peptide in each state (f_n, f_i, f_u) is given by

$$f_n = N/(N + I + U) = 1/(1 + K_{ni} + K_{nu}) \quad (2a)$$

$$f_i = I/(N + I + U) = K_{ni}/(1 + K_{ni} + K_{nu}) \quad (2b)$$

$$f_u = U/(N + I + U) = K_{nu}/(1 + K_{ni} + K_{nu}) \quad (2c)$$

The fractional signal change (S) as a function of denaturant concentration [D] is given by

$$S([D]) = (S_i K_{ni} + K_{nu})/(1 + K_{ni} + K_{nu}) \quad (3)$$

where S_i is a characteristic of the intermediate species. The equilibrium constants are dependent on the concentration of denaturant, and two models are used to describe this concentration dependence. The simplest model of Pace (model 1) assumes that the free energy is linearly related to the concentration of denaturant (*14*). The free energies between the conformational states are given by

$$\Delta G_{ni} = \Delta G_{0,ni} - m_{ni}[D] = -RT \ln K_{ni} \quad (4a)$$

$$\Delta G_{nu} = \Delta G_{0,nu} - m_{nu}[D] = -RT \ln K_{nu} \quad (4b)$$

where $\Delta G_{0,xy}$ is the conformational free energy in the absence of denaturant and m_{xy} is the slope of the linear dependence of ΔG_{xy} on [D]. An alternative extrapolation procedure (model 2) is based on the denaturant binding site model of Tanford (*15*). The free energy difference between the folded state and the intermediate state (ΔG_{ni}) or between the folded and unfolded states (ΔG_{ni}) as a function of denaturant concentration ([D]) is given by

$$\Delta G_{ni} = \Delta G^\circ_{ni} - \Delta N_{ni} RT \ln(1 + K_G[D]) \quad (5a)$$

$$\Delta G_{nu} = \Delta G^\circ_{nu} - \Delta N_{nu} RT \ln(1 + K_G[D]) \quad (5b)$$

where ΔG°_{xy} is the standard free energy between the conformational states, ΔN_{xy} is the change in binding site number required to bring about the transition, and K_G is the average association constant for the binding of denaturant (GuHCl) to the peptide−lipid complex. To reduce the number of variable parameters, K_G was set to 0.8 M^{-1}, the value recommended by Pace for proteins (*14*).

RESULTS

Peptide Unfolding in GuHCl. Figure 2 (upper panel) shows the effect of GuHCl on the fractional unfolding of peptides A-2 to E-14 complexed to egg PC SUVs, as determined by measurements of the CD ellipticity at 222 nm. Unfolding of the helical structure occurred at relatively low GuHCl concentrations (0−1.5 M) and was in general completed at concentrations above 1.5 M GuHCl. The lower panel of Figure 2 displays analogous data determined from measurements of tryptophan fluorescence intensity at 340 nm. Similar profiles were obtained when the total area under the emission curve was used. The average emission wavelengths of the tryptophan residues in the peptide−lipid complexes were also measured and in general showed negligible wavelength shifts (<2 nm) between 0 and 0.5 M GuHCl and an increase (A-2, 13; B-3, 2; C-7, 4; D-12, 0; E-14, 4) between 0.5 and 1.5 M GuHCl. Two lines of evidence indicate that the unfolding of the peptide−lipid complexes occurs with the involvement of one or more intermediates. First, the unfolding occurs in two steps, the first between 0 and 0.5 M GuHCl and the second between 0.5 and 1.5 M GuHCl. Second, the unfolding curves determined using circular dichroism are not coincident with those obtained from the fluorescence experiments. This difference is most clearly seen in the case of

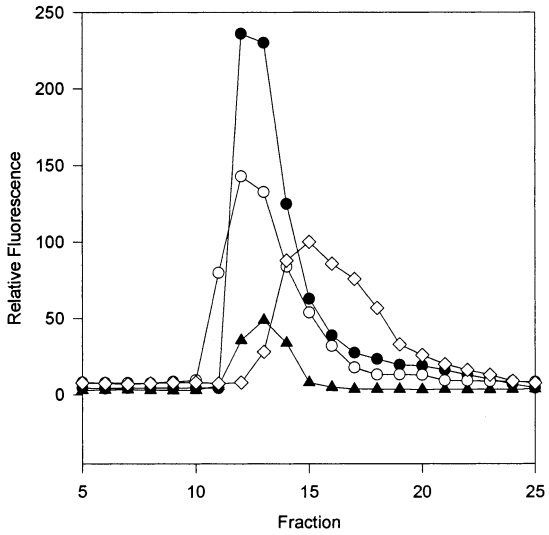

FIGURE 3: Size-exclusion gel chromatography of peptide C-7−SUV complexes on Sephadex G-25. The elution profiles are denoted as follows: egg PC SUVs (filled triangles), peptide 18C in the presence of 1.4 M GuHCl but in the absence of SUVs (unfilled diamonds), peptide 18C in the presence of SUVs (filled circles), and peptide 18C in the presence of egg PC SUVs and 1.4 M GuHCl (unfilled circles). The chromatograms in Figure 3 are representative for peptides A-2, B-3, D-12, and E-14.

the D-12 peptide−lipid complex (Figure 2) but holds for the other peptide−lipid complexes as well. Together, these observations suggest that a complex model of unfolding involving one or more intermediates is required to account for the experimental data.

Size-Exclusion Gel Chromatography. The unfolding experiments were carried out at relatively high mole ratios of lipid to peptide (200:1) to ensure that no free peptide was present in solution. However, we sought to establish whether the addition of GuHCl to the peptide−lipid complexes caused dissociation of the peptides from the lipid surface. The results of the gel filtration experiments for peptide C-7, using tryptophan fluorescence to monitor the eluant, are presented in Figure 3. In the absence (filled circles) and presence of denaturant (hollow circles) the peptide in peptide−egg PC SUV mixtures eluted with the egg PC SUVs, and there was no indication of material eluting at a position characteristic of the free peptide. Some broadening in the chromatogram of the peptide−lipid complexes in the presence of GuHCl was evident, however, which would obscure a quantitative evaluation of the amount of free peptide. Similar results were obtained for peptides A-2, B-3, D-12, and E-14 (data not shown). The small signal for the vesicles in the absence of peptide is due to vesicle scatter. Although the gel filtration data are largely consistent with the presence of intact peptide−lipid complexes in the presence of GuHCl, we cannot rule out the possibility of dissociation of a small amount (ca. 10%) of peptide from the complex on the basis of the chromatography data alone. We therefore used an alternative approach based on the observation of fluorescence energy transfer from the tryptophan residue in peptide C-7 to lipid-resident diphenylhexatriene in the lipid bilayers. This approach has been used to measure the amounts of free and bound protein in protein−membrane binding assays (*3*). Here, any dissociation of peptide−lipid complexes in the presence of GuHCl would be detected by a decreased rate of energy transfer. In the peptide−lipid complexes in the absence of GuHCl we measured an apparent rate of energy transfer of 0.2 ns^{-1} (obtained from the measured transfer efficieny of 39% and the published average fluorescence lifetime of 3.8 ns) to the diphenylhexatriene energy acceptors in the bilayer. In the presence of GuHCl, no change in energy transfer rate was observed (apparent energy transfer rate of 0.2 ns^{-1}), implying negligible dissociation of the peptide from the peptide−lipid complex.

Table 1: Thermodynamic Parameters Corresponding to a Three-State Model for the Unfolding of the Amphipathic Class A Peptides on the Surface Egg PC SUVs

	model 1[a]		model 2[b]	
peptide	ΔG_{ni}	ΔG_{nu}	ΔG_{ni}	ΔG_{nu}
A-2	0.7 ± 0.2	3.3 ± 0.2	0.7 ± 0.2	4.6 ± 0.3
B-3	1.7 ± 0.2	4.0 ± 0.3	1.7 ± 0.2	4.8 ± 0.4
C-7	1.2 ± 0.2	3.9 ± 0.3	1.2 ± 0.2	4.8 ± 0.4
D-12	1.3 ± 0.2	4.0 ± 0.2	1.2 ± 0.2	4.8 ± 0.3
E-14	1.1 ± 0.1	3.2 ± 0.2	1.2 ± 0.1	4.1 ± 0.3

[a] Free energy values obtained using the linear extrapolation method of Pace (eq 3 of text) and with concentration coefficients (*m*-values) common to the set of peptide−lipid complexes ($m_{nu} = 16.3$ kcal mol^{-1} M^{-1}; $m_{ni} = 3.8$ kcal mol^{-1} M^{-1}). [b] Free energy values in units of kcal/mol [native to intermediate transition (ΔG_{ni}); native to unfolded transition (ΔG_{nu})] obtained using the binding site model of Tanford (eq 4 in text) and with binding site parameters common to the five peptide−lipid complexes ($K_G = 0.8$ M^{-1}; $\Delta N_{ni} = 35$; $\Delta N_{nu} = 49$).

Data Fitting. The GuHCl unfolding curves generated from circular dichroism experiments were fitted to the three-state model described in Materials and Methods. Nonlinear least-squares fitting of the data to eq 2 was carried out in several stages. In the first stage each unfolding curve was fitted individually with all unknown parameters allowed to vary (S_i, $\Delta G_{0,ni}$, $\Delta G_{0,nu}$, m_{ni}, and m_{nu} in model 1 and S_i, $\Delta G°_{ni}$, $\Delta G°_{nu}$, ΔN_{ni}, and ΔN_{nu} in model 2). This procedure produced good fits, but analysis of the confidence intervals suggested that the parameters were poorly defined (results not shown) and we could not reliably distinguish differences in the stability of peptide−lipid complexes based on single fits alone. This is an expected consequence of having many interdependent parameters in the model (five parameters to fit a single biphasic transition curve). In the second stage of fitting, it was assumed that the parameters describing the dependence of denaturant concentration on the free energy (m_{ni} and m_{nu} in model 1 and ΔN_{ni} and ΔN_{nu} in model 2) were common to all peptide−lipid complexes and were therefore constrained in the analysis. Only the free energy values characteristic of each unfolding step were allowed to vary. This is a common assumption made in unfolding studies of mutant forms of soluble proteins (*9*). For peptides B-3, C-7, and E-14 where conservative amino acid replacements were made, this would be expected to be a reasonable first-order approximation. However, for peptides A-2 and D-12 where polar amino acids are replaced by nonpolar ones, this assumption should be considered approximate. It is noted that this procedure reduces the total number of variable parameters to 17 compared with ($5 \times 5 =$) 25 for the unconstrained analysis of the five peptide−lipid complexes as a whole. The parameters resulting from fitting eqs 1−5 (models 1 and 2) to the data are shown in Table 1, along with the 67% confidence interval widths. The parameters are reasonably determined, the confidence widths being of

the order of 10−20% for the free energy of the folded state with respect to the unfolded state (ΔG_{nu}).

The agreement between the experimental data and the fitted curves can be seen in Figure 2. The solid lines in the upper panel of Figure 2 represent the fit to the experimental data according to model 1. This model reproduces the overall contour of the experimental data reasonably well, given the constraints imposed. Model 2 gave comparably good fits (data not shown).

DISCUSSION

Interpretation and Modeling of the Experimental Data. We make three main assumptions in the interpretation of the experimental data. First, it is assumed that the peptides remain associated with the lipid−water interface during the denaturant-induced unfolding with no major changes in the mode of association of the peptides with the lipid surface. The results of the gel size-exclusion chromatography and fluorescence resonance energy transfer experiments establish that in the presence of the highest GuHCl concentration used (1.4 M) the peptides elute with the lipid and that no major dissociation of the peptides occurs. The changes in average wavelength of tryptophan emission are consistent with an increased exposure of the tryptophan residues to a more polar environment during peptide unfolding. In contrast, increases in lipid penetration of the peptide would result in opposite changes in average wavelength for one or more tryptophan residues. This was not observed. Therefore, the peptide unfolding is largely confined to the interfacial region of the lipid bilayer. Second, it is assumed that the denaturant does not perturb the structure of the lipid particle. Large structural changes in the lipid particle due to GuHCl can be excluded on the basis of reports that egg PC vesicles do not leak entrapped carboxyfluorescein when incubated with up to 3 M GuHCl (*16*). We observed no change in fluorescence emission of the lipid-resident diphenylhexatrieene probe, consistent with the lack of large structural perturbations to the hydrocarbon core. Differential scanning calorimetry of synthetic phospholipids also shows that the bilayer structure is largely maintained in the presence of GuHCl as evidenced by the presence of a defined gel-crystalline phase transition (*17*). The small concentration range of denaturant used in the present work (0−1.4 M GuHCl) suggests that any denaturant-induced perturbations to overall vesicle structure will be small. However, it is clear from the observed peptide unfolding that the GuHCl must perturb the environment local to the membrane peptides via direct binding to the peptide (*15*) or membrane interface (*17*) or via indirect chaotropic effects on bulk solvent properties. Third, the assumption is that there are only three conformational states of the peptide on the lipid surface. The model treats the intermediate as a single species. This assumption can be tested by comparing independent measures of the unfolding process. The fluorescence changes resulting from GuHCl-induced unfolding are also biphasic, are in qualitative agreement with the CD measurements, and can also be modeled on the basis of a three-state model (fits not shown). However, a quantitative comparison was not attempted because fluorescence does not report on global conformations but is influenced by local interactions with amino acid side chains and the surrounding solvent.

A failure of any of the above assumptions would reduce the reliability of the derived thermodynamic parameters. Failure of the first assumption would remove physical significance from the derived parameters. A failure of the second assumption would make interpretation in terms of the conformational stability of the peptide meaningless but would be useful in defining a stability of the peptide−lipid complex. A failure of the third assumption would strip all meaning from the parameters involving the intermediate state but provide an approximate lower limit for the stability of the native state with respect to the unfolded state.

Stability and Structure of the Native and Intermediate Lipid-Associated Peptide States. The membrane-bound forms of the peptides shown in Figure 1 have been studied previously by optical spectroscopy. Using various fluorescence parameters, the position-dependent micropolarity of the environment surrounding the tryptophan residue at each site was determined and found to be consistent with that of an amphipathic peptide lying parallel to the lipid surface (*10*). Thus, the tryptophan on the polar face of peptide D-12 was found to be in a polar, water-exposed environment. Tryptophans on the nonpolar face of the helix (B-3, C-7, E-14) were in a nonpolar water-shielded low dielectric environment, while the tryptophan near the polar−nonpolar interface of the amphipathic helix (A-2) was in an environment of intermediate polarity and water exposure. An interfacial location for an N- and a C-terminally blocked version of peptide A-2 in fluid multilayers was independently confirmed from X-ray diffraction studies (*13*).

According to the present three-state model for denaturant-induced peptide unfolding the stability of the membrane-bound native state with respect to the membrane-bound unfolded state of the set of peptides lies in the range 3.2−4.0 kcal/mol (model 1) and 4.1−4.8 kcal/mol (model 2). The lower set of values obtained using model 1 is an expected consequence of using the linear extrapolation method of Pace compared to the binding site model of Tanford (model 2) (*9*). An important concern is whether the thermodynamic parameters are quantitatively reasonable, given the assumptions made in the modeling and analysis. According to the thermodynamic model of White and co-workers the partitioning free energy of a peptide into a bilayer interface is equal to the sum of the free energies due to partitioning of the amino acid side chains into the bilayer and a contribution due to the folding of the partitioned peptide from an unfolded conformation to a folded one (*5*, *7*). If our unfolding data are reasonable, then our predicted free energy of partitioning should be close to the experimentally determined one. From the model of peptide A-2 at a lipid interface (*10*, *13*) and the whole residue partitioning scale of Wimley and White (*5*), we estimated a free energy of −3.9 kcal/mol for the partitioning of the hydrophobic face of peptide A-2 into lipid bilayers. Combined with the unfolding data, from which we determined a folding free energy of −3.3 to −4.6 kcal/mol, we predict a peptide partitioning free energy of −7 to −8.5 kcal/mol. This estimate agrees remarkably well with literature values (*6*) and our data (−7.6 kcal/mol) for the partitioning of peptide A-2 into egg PC lipid bilayers. The level of agreement is perhaps surprising, given that the extrapolation procedures used for extracting the free energies for unfolding were derived for soluble proteins (*9*, *14*, *15*) and not peptide−lipid complexes. Thus we consider m_{ni} and m_{nu} in model 1

and ΔN_{ni} and ΔN_{nu} in model 2 as largely empirical and postpone detailed interpretation of these parameters until a greater mechanistic understanding of the process of GuHCl-induced unfolding is reached.

An important question is whether substitution of tryptophan residues at specific sites has a major effect on the apparent stability of the peptide on a lipid surface. Comparing the stabilities of the peptides, it can be seen that the effect of tryptophan substitution at different sites has a relatively minor effect on the stability of the native state. The largest difference in stabilities is observed between peptides D-12 and E-14 (model 1, $\delta\Delta G_{nu} = 0.8 \pm 0.4$ kcal/mol; model 2, $\delta\Delta G_{nu} = 0.7 \pm 0.6$ kcal/mol) and is of borderline significance at the 67% confidence level. Moreover, substitution of the tryptophan in the polar or nonpolar face of the peptide does not seem to have a marked effect on the conformational stability of the peptides on the lipid surface. This is consistent with preliminary partitioning studies which show that the binding of peptides A−E to membranes occurs with similar affinity (Clayton and Sawyer, unpublished observations).

Both methods of analysis yield better agreement with respect to the Gibbs free energy difference between the folded and the intermediate state. The values obtained are consistent with a model in which the intermediate state is closer in Gibbs energy to the folded state than to the unfolded state (cf. Table 1). The intermediate state has approximately 50−80% of the conformational stability of the folded state. To examine whether the intermediate state retains some of the amphipathic characteristics of the native amphipathic helix, the average emission wavelength of peptides A-2 to E-14 in the lipid-bound native state were compared with the corresponding values for the intermediate, as determined from the fluorescence spectra obtained under conditions under which over 90% of the intermediate state is populated. We have shown previously that the average emission wavelength is a good indicator of the transbilayer distribution of the tryptophan residues in these lipid−peptide complexes and in the native state reflects the expected micropolarity pattern for an amphipathic helix lying parallel to a membrane interface (*10*). The fluorescence spectra of the intermediates of the set of peptide−lipid complexes were found to undergo very small changes in average fluorescence wavelength with respect to the corresponding native forms (<2 nm; results not shown). This suggests that both the magnitude and pattern of micropolarity of the tryptophan residue in the native state are largely maintained in the intermediate state for this family of peptide−lipid complexes. However, structural perturbations are clearly evident from the changes in circular dichroism (backbone secondary structure) and from the changes in tryptophan fluorescence intensity (which reflect the nature of quenching interactions with solvent or proximal amino acid side chains). We propose that the intermediate is also an amphipathic structure with respect to tryptophan side chain disposition relative to the lipid−water interface but has an altered structure. This is in line with a molecular dynamics simulation of the folding of an ideally amphipathic helix at a water−hexane interface which showed that nonhelical backbone structures could be populated which still maintained the amphipathic distribution of polar and nonpolar side chains (*18*). Presumably the properties of the lipid interface, particularly the steep transbilayer polarity gradient, stabilize intermediate forms of polypeptides with high hydrophobic moments that fold/unfold via an amphipathic pathway.

Comparison with Other Studies. There have been relatively few quantitative studies on the conformational stability of α-helical peptides on membrane interfaces, as compared with the corresponding studies of water-soluble polypeptides. Venkatachalapathi et al. examined the conformational stability of peptide A-2−dimyristoylphosphatidylcholine discoidal complexes using GuHCl as the denaturant (*19*). Their reported value of ΔG_{nu} (1.7 ± 0.2 kcal/mol) is significantly different from the value obtained in the present work (4.6 ± 0.3 kcal/mol). The most likely source of this discrepancy is the assumption of a two-state unfolding model (*19*) that will underestimate ΔG_{nu} in a system with stable intermediates (*9*). White and co-workers have used a novel method to determine the contribution of peptide helicity to the free energy of partitioning of the helical bee venom peptide melittin on the surface of POPC vesicles. They obtained a value of 5.0 ± 0.7 kcal/mol by comparing the partition free energies of a native α-helix-forming melittin sequence and a melittin sequence with peptides with D-amino acids introduced to prevent the formation of an α-helix on the membrane surface (*7*). If it is assumed that a two-state model is applicable and that both melittin sequences have identical conformational free energies in buffer, then the above estimate can be considered a measure of the conformational stability of the melittin helix on the POPC vesicle surface. Reijngoud and Phillips (*16*) used denaturant-based techniques similar to those employed in the present study to determine the conformational stability of apolipoprotein A-1 on dimyristoylphosphatidylcholine vesicles and obtained a value of 5.5 ± 1.2 kcal/mol using a two-state model. Apolipoprotein A-IV has also been studied and found to have a conformational stability of 6.3 kcal/mol on egg phosphatidylcholine vesicles (*20*). The similarity in membrane-bound conformational stabilities between the apolipoproteins and the class A helices studied here may be coincidental but is consistent with the notion that the lipid-bound apolipoprotein structure gains much of its stabilization from its α-helical amphipathic domains.

The observation that the peptide can exist in an unfolded state on the bilayer surface is important when considering the mechanism involved in the association of the peptide with the lipid structure. One view is that although the peptide is unfolded in solution, it is nevertheless in equilibrium with a folded α-helical state that preferentially associates with the bilayer surface, so shifting the equilibrium in favor of the folded form. The alternative view is that folding is not a prerequisite for association with lipid but only occurs after the association reaction. Our finding that the unfolded peptide can remain associated with the lipid surface indicates that this latter view is a distinct possibility.

Much remains to be learned about the factors influencing the conformational stability of polypeptides on membrane interfaces. It is envisaged that techniques such as denaturant unfolding will add to existing approaches and prove useful in examining the effects of amino acid sequence, hydrophobic moment, and lipid composition on the conformational stability of de novo designed membrane−peptides as well as helping to unravel the rules of membrane−protein conformational stability in naturally occurring systems.

ACKNOWLEDGMENT

We thank Dr. Allen Minton for useful discussions and for providing algorithms for data analysis.

REFERENCES

1. Popot, J.-L., and Engelman, D. M. (2000) Helical membrane protein folding, stability and evolution, *Annu. Rev. Biochem. 69*, 881−922.
2. Booth, B. P., and Curran, A. R. (1999) Membrane protein folding, *Curr. Opin. Struct. Biol. 9*, 115−121.
3. Soekarjo, M., Eisenhower, M., Kuhn, A., and Vogel, H. (1996) Thermodynamics of the membrane insertion process of the M13 procoat protein, a lipid bilayer traversing protein containing a leader sequence, *Biochemistry 35*, 1232−1241.
4. Kleinschmidt, J. H., and Tamm, L. (1999) Time-resolved distance determination by tryptophan fluorescence quenching: probing intermediates in membrane protein folding, *Biochemistry 38*, 4996−5005.
5. White, S. H., and Wimley, W. C. (1998) Hydrophobic interactions of peptides with membrane interfaces, *Biochim. Bioiphys. Acta 1376*, 339−352.
6. Gazzara, J. A., Phillips, M. C., Lund-Katz, S., Palgunachari, M. N., Segrest, J. P. Anatharamaiah, G. M., and Snow, J. W. (1997) Interaction of class A amphipathic helical peptides with phospholipid unilamellar vesicles, *J. Lipid Res. 38*, 2134−2146.
7. Ladokhin, A. S., and White, S. H. (1999) Folding of amphipathic alpha-helices on membranes: Energetics of helix formation by melittin, *J. Mol. Biol. 285*, 1363−1369.
8. Wieprecht, T., Apostolov, O., Beyermann, M., and Seelig, J. (1999) Thermodynamics of the alpha-helix-coil transition of amphipathic peptides in a membrane environment: Implications for the peptide-membrane binding equilibrium, *J. Mol. Biol. 294*, 785−794.
9. Pace, C. N. (1986) Determination and analysis of urea and guanidine hydrochloride denaturation curves, *Methods Enzymol. 131*, 266−280.
10. Clayton, A. H. A., and Sawyer, W. H. (1999) The structure and orientation of class-A amphipathic peptides on a phospholipid bilayer surface, *Eur. Biophys. J. 28*, 133−141.
11. Clayton, A. H. A., and Sawyer, W. H. (1999) Tryptophan rotamer distributions in amphipathic peptides at a lipid surface, *Biophys. J. 76*, 3235−3242.
12. Clayton, A. H. A., and Sawyer, W. H. (2000) Site-specific tryptophan dynamics in class A amphipathic helical peptides at a phospholipid bilayer interface, *Biophys. J. 79*, 1066−1073.
13. Hristova, K., Wimley, W. C., Mishra, V. K., Anatharamiah, G. M., Segrest, J. P., and White, S. H. (1999) An amphipathic alpha-helix at a membrane interface: A structural study using a novel X-ray diffraction method, *J. Mol. Biol. 290*, 99−117.
14. Pace, C. N., and Vandenburg, K. E. (1979) Determining global protein stability—guanidine hydrochloride denaturation of myoglobin, *Biochemistry 18*, 288−292.
15. Aune, K. C., and Tanford, C. (1969) Thermodynamics of the denaturation of lysozyme by guanidine hydrochloride, *Biochemistry 8*, 4586−4590.
16. Reijngoud, D. J., and Phillips, M. C. (1982) Mechanism of dissociation of human apolipoprotein A−I from complexes with dimyristoylphosphatidylcholine as studied by guanidine hydrochloride denaturation, *Biochemistry 21*, 2969−2976.
17. Jain, M. K., and Wu, N. M. (1977) Effect of small molecules on the dipamitoyl lecithin liposomal bilayer. III. Phase transition in lipid bilayer, *J. Membr. Biol. 34*, 157−201.
18. Chipot, C., Maigret, B., and Pohorille, A. (1999) Early events in the folding of an amphipathic peptide: A multi-nanosecond molecular dynamics study, *Proteins 36*, 383−399.
19. Venkatachalapathi, Y. V., Phillips, M. C., Epand, R. M., Epand, R. F., Tytler, E. M., Segrest, J. P., and Anatharamaiah, G. M. (1993) Effect of end group blockage on the properties of class A amphipathic helical peptides, *Proteins 15*, 340−359.
20. Weinberg, R. B., and Jordan, M. K. (1990) Effects of phospholipid on the structure of human apolipoprotein-A-IV, *J. Biol. Chem 265*, 8081−8086.

BI020439Z